Liquid Crystals
Publication details, including instructions for authors and subscription information:
http://www.informaworld.com/smpp/title~content=t713926090

Fine structure of the repolarization current in the B 2 phase of a banana compound

M. I. Barnik; L. M. Blinov; N. M. Shtykov; S. P. Palto; G. Pelzl; W. Weissflog

Online publication date: 11 November 2010

To cite this Article Barnik, M. I. , Blinov, L. M. , Shtykov, N. M. , Palto, S. P. , Pelzl, G. and Weissflog, W.(2002) 'Fine structure of the repolarization current in the B 2 phase of a banana compound', Liquid Crystals, 29: 4, 597 — 603
To link to this Article: DOI: 10.1080/02678290110114873
URL: http://dx.doi.org/10.1080/02678290110114873

LIQUID CRYSTALS, 2002, VOL. 29, NO. 4, 597–603

Taylor & Francis
Taylor & Francis Group

Fine structure of the repolarization current in the B_2 phase of a banana compound

M. I. BARNIK, L. M. BLINOV*, N. M. SHTYKOV, S. P. PALTO
Institute of Crystallography, Russ. Acad. Sci., Leninsky prosp. 59, Moscow 117333, Russia

G. PELZL and W. WEISSFLOG
Institute of Physical Chemistry, Martin Luther University Halle-Wittenberg, Mühlpforte 1, 06108 (S), Germany

(*Received 17 March 2001; in final form 29 October 2001; accepted 31 October 2001*)

A detailed study of the field induced polarization switching has been carried out over the whole temperature range of the antiferroelectric B_2 phase of a banana-shaped compound, the tetradecyl homologue ($n = 14$) of the series 4-chloro-1,3-phenylene bis[4-(4-*n*-alkylphenylimino)benzoate]s. The fine structure of the current response oscillograms was attributed to the field switching of two antiferroelectric subsystems, most probably the racemic and homogeneously chiral domains which, according to the Boulder group, appear as a result of the spontaneous breaking of mirror symmetry. The temperature and field dependences of polarization as well as switching times and the corresponding viscosity of the substance have been measured.

1. Introduction

Recently liquid crystalline polar [1], antiferroelectric [2–4] and ferroelectric [5] compounds have been designed which, in contrast to the well known liquid crystalline ferro- and antiferro-electrics [6, 7], are composed of achiral molecules and show high values of the electric polarization (see review [8]). Among these new compounds, those consisting of banana-shaped molecules [2, 4, 5] attract great interest from a fundamental viewpoint because they spontaneously form macroscopic chiral domains due to the local breaking of mirror symmetry [9]. In addition, in the B_2 antiferroelectric phase of banana-shaped compounds, the polarization and optical transmission can be switched very quickly, and therefore such compounds are very promising for application in display technology.

The B_2 phase is a tilted smectic phase with liquid-like in-plane molecular order (see [4] and references therein). According to the model developed by the Boulder group [9], in the B_2 phase, each of the chiral domains, left (HL) and right (HR), are present in equal amounts. The ground state of the racemic R-domains is synclinic, i.e. the molecules are tilted with the same azimuthal angle, and the direction of the in-plane polarization alternates between neighbouring layers. Under an electric field exceeding a certain threshold, the polarization follows the field direction and the structure becomes anticlinic with the tilt direction alternating between neighbouring layers and uniform polarization. The ground state of the HL and HR states is anticlinic (but also with an alternating direction of the local polarization) and the field induced state is synclinic, as in the SmC* phase, with uniform macroscopic polarization along the field direction. In other words, the field switches the symmetry from I to C_{2v} in the case of racemic domains, and from D_2 to C_2 in the case of homogeneously chiral domains.

In general, the kinetics of the two field induced changes in symmetry should be different, and the oscillograms of the repolarization current are expected to be more complex than those observed in conventional antiferroelectrics. To date, only qualitative results on the kinetics of the polarization reversal are available [10–13] in which only two current peaks have been reported, typical of antiferroelectrics switched by a triangular voltage wave form (in [14] an additional peak in the current oscillogram is seen and other oscillograms with multiple peaks are mentioned without explanation). The aim of the present paper is to carry out a more detailed investigation of the field induced polarization kinetics, and to study the fine structure of multi-peak oscillograms of the repolarization current as a function of an applied field over a wide temperature range in the B_2 phase composed of banana-shaped molecules.

* Author for correspondence; e-mail: lcl@ns.crys.ras.ru

Liquid Crystals ISSN 0267-8292 print/ISSN 1366-5855 online © 2002 Taylor & Francis Ltd
http://www.tandf.co.uk/journals
DOI: 10.1080/02678290110114873

2. Experimental

The compound studied is the tetradecyl homologue ($n = 14$) of the series 4-chloro-1,3-phenylene bis-[4-(4-*n*-alkylphenylimino)benzoate]s reported earlier [12]. It is crystalline at room temperature, and shows the B_2 phase in the range 75–127°C. The transition to the isotropic phase at 127°C is accompanied by an enthalpy change 14.9 kJ mol^{-1}, and thus it is evidently a first order transition. The B_2 phase optical textures observed in [12] were dependent on the cell treatment and thermal pre-history, and the field switched polarization measured was about 500 nC cm^{-2}. Electro-optical studies showed clearly the three types of domain described above as R, HL and HR.

The cell used consists of two ITO glass plates separated by teflon strips to form a 10 μm gap (measured by the capacitance of the empty cell) with an electrode overlapping area of 4.1×4.2 mm^2. The inner surfaces of the cell were covered by polyimide layers and rubbed unidirectionally. The cell was filled with liquid crystal in the isotropic phase. In our case, the optical textures were also dependent on the cell treatment, and especially on whether the field was applied during the cooling cycle or not.

The measurements of the repolarization current were carried out using triangular voltage pulses and standard circuitry with a cell load resistor $R_L = 2$ kΩ. The voltage drop over R_L was delivered to the input of the multimedia card of an IBM computer where the oscillograms were measured and stored using a virtual digital oscilloscope (the PhysLab software developed by S.P. Palto; in the new version corrections have been introduced to expand the card frequency range). Where necessary, e.g. for measurements of short pulse fronts or, by contrast, long period wave forms, a standard memory oscilloscope was used.

3. Theoretical background

In the triangle-wave technique [15] an electric field $\mathbf{E}(t)$ with a triangular waveform of amplitude $\mathbf{E}_m$ and frequency f is applied to a cell, filled with the liquid crystal under investigation, and the current $i(t)$ through the cell is measured. The current density $j(t)$ through the cell is given by

$$j(t) = \sigma \mathbf{E}(t) + \frac{\partial D(t)}{\partial t} \tag{1}$$

where $D(t)$ and σ are the electric displacement and conductivity along the electric field direction, respectively. In the case of polar liquid crystals $D(t)$ can be given by

$$D(t) = \varepsilon_0 \mathbf{E}(t) + P(t) = \varepsilon_0 \varepsilon(t) \mathbf{E}(t) + \mathbf{P}_{sw}(t). \tag{2}$$

Here $\varepsilon_0 = 8.85 \times 10^{-12}$ F m^{-1} is the permittivity of vacuum, $\mathbf{P}(t)$ is the total electric polarization, $\varepsilon(t)$ is an anisotropic relative 'background' permittivity without the contribution of the spontaneous polarization and $\mathbf{P}_{sw}(t)$ is the field dependent switched component of the spontaneous polarization (averaged over the cell). The total current $i(t)$ through the cell is proportional to the current density $j(t)$, and electrode overlapping area A:

$$i(t) = A\left[\sigma \mathbf{E}(t) + \varepsilon_0 \varepsilon(t) \frac{d\mathbf{E}(t)}{dt} + \varepsilon_0 \frac{d\varepsilon(t)}{dt} \mathbf{E}(t) + \frac{d\mathbf{P}_{sw}(t)}{dt}\right] \tag{3}$$

or

$$i(t) = A\left\{\sigma \mathbf{E}(t) + \left[\varepsilon_0 \varepsilon(t) + \varepsilon_0 \frac{d\varepsilon}{d\mathbf{E}} \mathbf{E}(t) + \frac{d\mathbf{P}_{sw}}{d\mathbf{E}}\right] \frac{d\mathbf{E}(t)}{dt}\right\}. \tag{4}$$

One can see that the total current consists of the resistive current due to ion flow and two currents due to dipole realignment. The first dipole current (the 2nd and the 3rd terms) is determined by the background permittivity ε of the liquid crystal and the second one (the 4th term) is due to the spontaneous polarization $\mathbf{P}_{sw}$. For an electric field $\mathbf{E}(t)$ with a triangular waveform, the time derivative is $d\mathbf{E}/dt = \pm 4\mathbf{E}_m f$, where signs (+) and (−) correspond to one-half period of the wave for increasing or decreasing field. Finally, for the triangular waveform

$$i(t) = A\left\{\sigma \mathbf{E}(t) \pm 4\mathbf{E}_m f\left[\varepsilon_0 \varepsilon(t) + \varepsilon_0 \frac{d\varepsilon}{d\mathbf{E}} \mathbf{E}(t) + \frac{d\mathbf{P}_{sw}}{d\mathbf{E}}\right]\right\}. \tag{5}$$

To see the contributions of the different terms in $j(t)$, consider a model antiferroelectric liquid crystal (AFLC) cell without conductivity and with the voltage dependence of ε and $\mathbf{P}_{sw}$ shown in figure 1. The dielectric term includes a field independent part $\varepsilon = 4$ and also can include a field dependent contribution (e.g. originating

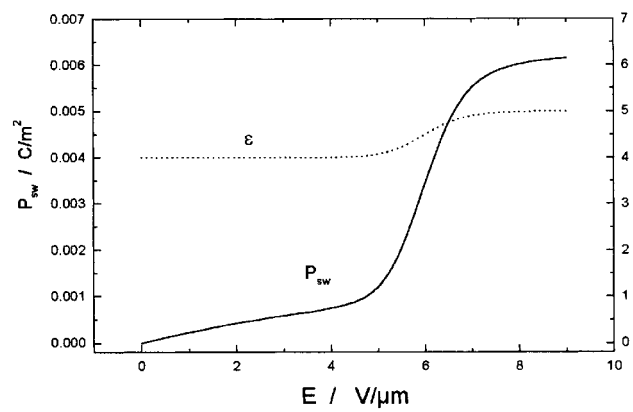

Figure 1. Field dependence of parameters ε and $\mathbf{P}_{sw}$ for a model antiferroelectric liquid crystal.

from the dielectric anisotropy), with a component of ε along the cell normal dependent on the director switching process. This process is modelled by a steep field induced increase in ε with $\delta\varepsilon = 1$. The field dependent antiferroelectric polarization (with saturation value $\mathbf{P}_s \approx 600\ \mathrm{nC\,cm^{-2}}$) is modelled by the curve with two inflection points, an initial slope at low fields (lower than the apparent threshold) is deliberately exaggerated in order to see its influence on the shape of the repolarization current oscillogram.

The result of $j(t)$ modelling with a 10 µm thick cell is shown in figure 2. Repolarization current oscillograms for different applied voltages show two peaks typical of AFLCs and a small bump in between coming from the slope of the $\mathbf{P}(\mathbf{E})$ curve at low fields, see figure 1. The dotted curve shows the contribution of the ε-terms in equation (5) at the maximum voltage applied (± 90 V). For the assumed values of $\delta\varepsilon$ and $\mathbf{P}_s$ the contribution of the $\delta\varepsilon$ term can be neglected.

4. Results and discussion

Figure 3 (*a*) displays a repolarization current oscillogram recorded directly from the digital oscilloscope screen (voltage amplitude $U_m = \pm 90$ V, frequency $f = 50$ Hz). It is taken after cooling the cell from the isotropic phase to 123°C with no field applied. Three distinct peaks and an additional shoulder on the first peak are clearly seen. The oscillogram also shows a contribution from the cell conductivity σE schematically indicated by a dotted line. The specific resistance of the substance estimated from σ in the isotropic phase ($T = 130.5$°C) from another oscillogram is reasonably good $\rho \approx 2 \times 10^9\ \Omega$ cm; in the B_2 phase it is approximately double.

The time independent component originates from the zero-field capacitance of the cell, i.e. from the term $\varepsilon_0\varepsilon(\mathbf{E} = 0)$ in equation (5) and contributes to a current I_c which provides the well known permanent pedestal with the amplitude dependent on frequency f and field amplitude $\mathbf{E}_m$. As usual it can easily be subtracted; in figure 1 (*a*) it is very small. The field dependent part of the background ε is unknown, but for our substance should be negligible due to a very high contribution of the term $d\mathbf{P}_{sw}/d\mathbf{E}$ to the total current.

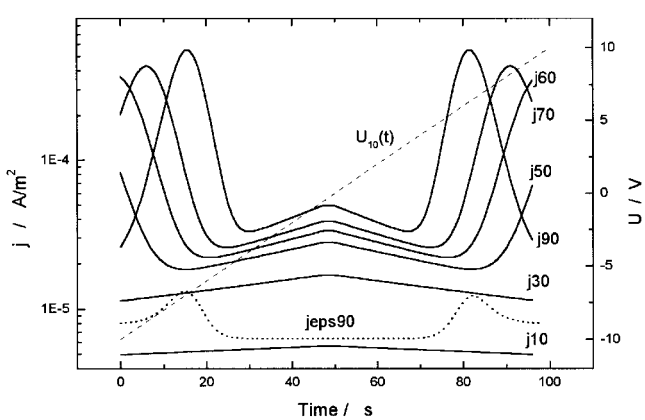

Figure 2. Repolarization current oscillograms for different applied voltages. The dotted curve shows the contribution of pure dielectric terms (both ε and $\delta\varepsilon$) in equation (5) at the maximum voltage applied (± 90 V). The dashed curve shows the applied field waveform.

After subtracting the capacitive I_c and resistive I_r components of the current we obtain the oscillogram shown in figure 3 (*b*)—only for increasing voltage due to the similarity of the positive and negative current response in figure 3 (*a*). Evidently the current oscillogram is more complicated than the model ones shown in figure 2. It is well approximated (dotted line) by five Gaussians (curves 1–5). The first two Gaussians (1, 2) correspond to decreasing absolute field magnitude $|\mathbf{E}|$, when the field only slightly counteracts the free relaxation of polarization. The second pair (Gaussians 4, 5) corresponds to increasing $|\mathbf{E}|$, when the field competes with the elasticity of the system. Therefore the oscillogram is not expected to be symmetric with respect to the zero-field point. The fifth peak (3) is necessary to describe a finite current at zero field (see later).

The total integral of the dotted curve in figure 3 (*b*) corresponds to $2A\mathbf{P}_{sw}$ where $A = 0.17\ \mathrm{cm^2}$ is the electrode overlapped area and $\mathbf{P}_{sw}$ is the polarization switched (which, by analogy with a ferroelectric, may be treated with some caution, as a spontaneous polarization). The value found from that integral is $\mathbf{P}_{sw} = 408\ \mathrm{nC\,cm^{-2}}$, which is somewhat lower than the value reported in [12]. It is informative to analyse the partial contributions to the total area, obtained from the fitting procedure, see the table.

The current oscillogram in figure 3 (*b*) may be interpreted as follows. The four sharp peaks point to the existence of two different antiferroelectric sub-systems with different threshold voltages for switching: external peaks 1 and 5 are associated with the sub-system with higher threshold and peaks 2 and 4 to the lower threshold one. In this case, the $\mathbf{P}_{sw}(\mathbf{E})$ curve is more complicated than the model curve in figure 1: it should have an additional inflection point, although probably difficult to observed. There is also a broad peak, 3, located close to the zero-voltage.

From the table we can see the reason for the asymmetry of the oscillogram with respect to the zero field point: the sum of areas under curves 1 and 2 ($\mathrm{Area}_{1+2} = 206\ \mathrm{nC\,cm^{-1}}$) is almost equal to the area under curves 3, 4 and 5 ($\mathrm{Area}_{3+4+5} = 202\ \mathrm{nC\,cm^{-1}}$), therefore a broad peak 3 should be attributed to a process controlled by the increasing part of the field $|\mathbf{E}|$. The nature of peak 3 is not very clear. At first, we believed that the reason for a finite current plateau between the first (1, 2) and

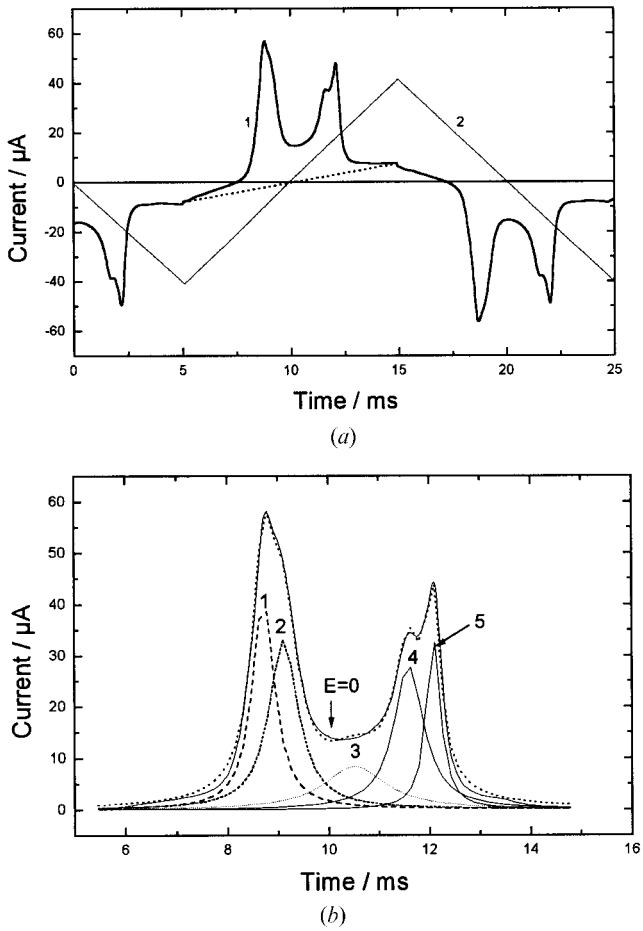

Figure 3. (*a*) Oscillogram of the current response (1) to triangular wave voltage (2) at $T = 123°C$ (voltage amplitude $U_m = \pm 90$ V, frequency $f = 50$ Hz). The cell was cooled from the isotropic phase without the field applied. Conductivity contribution is shown by a dotted line. (*b*) A part of the same oscillogram (solid line) decomposed into five Gaussians after subtracting the capacitive and resistive components of the current (curves with numbers). The resulting curve is shown by a dotted line.

Table. Parameters of the five Gaussian peaks used to fit the oscillogram in figure 3 (*b*).

Peak	Normalized area under a peak nC cm^{-2}	Position ms	Width ms	Height μA
1	100	8.73	0.53	41.3
2	106	9.03	0.69	33.1
3	57.5	10.53	1.47	8.5
4	93	11.6	0.71	28.1
5	51.5	12.09	0.33	33.8

second (4, 5) pairs of peaks (that is of peak 3) is related to the insufficiently long period of the triangular voltage. However, decreasing the frequency to 2 Hz does not result in its decrease. In addition, at reduced frequency it becomes similar to the bump shown in figure 2. Therefore, most probably peak 3 points to some initial thresholdless stage of the field induced polarization switching. It might be, for example, related to some surface phenomenon or to irregularities at the boundaries of different types of domain. Similar untypical antiferroelectric switching may be seen in the hysteresis curve shown in [16] for another banana-shaped compound.

At this stage we may tentatively assume that the two antiferroelectric sub-systems are the same racemic (R) and homogeneously chiral (HR and HL) domains discussed above; the two chiral types must have the same kinetics and contribute to the same subsystem. We can also compare the partial polarizations related to each sub-system. Assuming that the area of peak 3 belongs to inner peak 4, we find $\text{Area}_{1+5} = 151.5$ nC cm^{-2} for outer peaks and $\text{Area}_{2+4+3} = 256$ nC cm^{-2} for inner peaks. Therefore, for this particular texture, 'the inner peak system' contributes more significantly to the total polarization.

The temperature variation of the current oscillograms is shown in figure 4 where, for simplicity, only six curves are displayed. In this case, the cell was cooled from the isotropic phase under an applied voltage of $U_m = \pm 95$ V, and the texture was different from that for figure 3. In the isotropic phase ($T = 130°C$), only the capacitance and conductivity contributions are seen, as already discussed above. In the B_2 phase, now only three distinct peaks are seen; the shoulder 2 corresponding in figure 3 to the decreasing $|\mathbf{E}|$ seems to be merged with the first peak. Now the curves may be fitted using only four (for 120.5 and 107.5°C) or even three (curve for 71.5°C) Gaussians. The maxima of the remaining peaks considerably change with temperature. For example, close

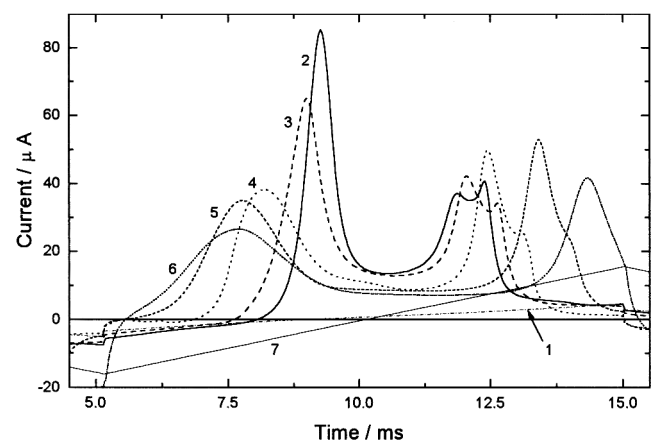

Figure 4. Oscillograms of the current response to triangular wave voltage at six different temperatures, T°C: 130 (1), 122 (2), 112.5 (3), 99.5 (4), 81.5 (5) and 71.5 (6). Voltage amplitude $U_m = \pm 95$ V, frequency $f = 50$ Hz (7). The cell was cooled from the isotropic phase with $U_m = \pm 95$ V voltage applied.

to the isotropic phase ($127°C > T > 115°C$) the current magnitude for the last peak **c** is higher than that of the previous one **b**, but with decreasing T down to 107.5°C, the situation changes to the opposite. However, the ratio of the areas under the corresponding peaks is almost unchanged $\mathbf{P}_b/\mathbf{P}_c \approx 2.5$–2.6. With decreasing temperature the last two peaks merge into one, see the curve for 71.5°C.

The total area under the current oscillogram changes only slightly with temperature; see figure 5. The two curves taken for decreasing and subsequent increasing temperature are almost identical. The switched polarization is practically constant in the range 70–110°C (slight deviations at $T < 80°C$ are related to some uncertainty in subtracting the conductivity contribution). However, an inflection point of the $\mathbf{P}_{sw}$ curve at $T_I \approx 15°C$ is very clear and accompanied by some change in the optical texture of the cell, although no changes were seen in the X-ray patterns. This probably involves a kind of textural transition caused, for example, by a change in anchoring conditions. It is interesting that a similar inflection point was observed in the B_2 phase of another compound [16]. At the transition to the isotropic phase the polarization abruptly decreases, clearly showing a strong first order phase transition.

Figure 6 shows the voltage dependence of the repolarization current oscillograms at a fixed temperature 122°C. We can see how the fine structure of the peaks develops with increasing voltage when the switching process becomes faster. The field dependence of the polarization $\mathbf{P}_{sw}$ (a current integral with I_c and I_r contributions subtracted) is shown in figure 7 (122°C, 50 Hz, cooling without field). This dependence is taken from 26 oscillograms (the number of points in the figure) taken first with increasing, then with decreasing voltage amplitude. The dependence shows a kind of a hysteresis, suggesting some texture difference before and after application of the maximum field. Only a weak repolarization current can be measured at $U_m < \pm 40$ V, showing some threshold-less switching which seems to be responsible for the Gaussian peak 3 in the switching current oscillogram, figure 3(*b*). Almost the same behaviour was observed for the cell cooled from the isotropic phase with voltage ± 95 V applied.

We also present the field dependence of $\mathbf{P}_{sw}$ in the form of the classical Sawyer-Tower loops by integrating the net polarization current time dependence, shown for example in figure 3(*b*), and plotting the integral as a function of the applied voltage. In this way we should see a double hysteresis characteristic of an antiferroelectric. An example is shown in figure 8 ($T = 123.5°C$).

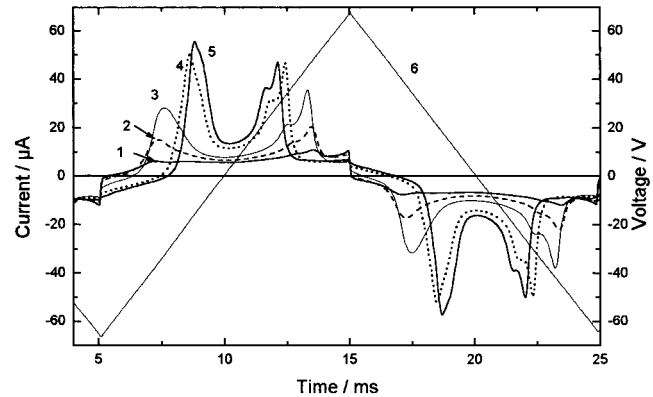

Figure 6. Oscillograms of the current response to triangular wave voltage at five different amplitudes U_m, V: 50 (1), 55 (2), 65 (3), 85 (4) and 90 (5); ($T = 122°C$, $f = 50$ Hz). Voltage form (for $U_m = \pm 65$ V) is also shown (6). The cell was cooled from the isotropic phase with $U_m = \pm 95$ V voltage applied.

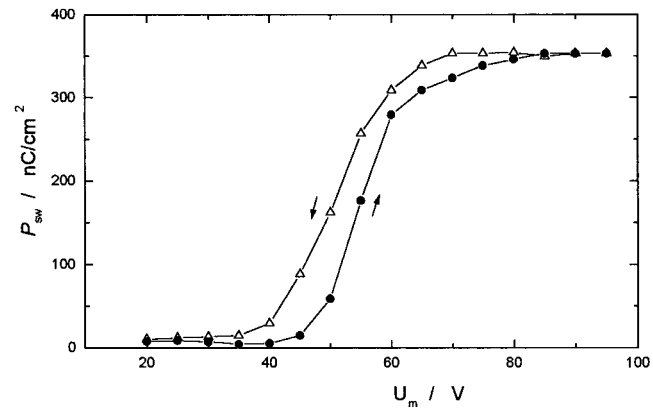

Figure 7. Voltage dependence of switched polarization $\mathbf{P}_{sw}$ (I_c and I_r contributions are subtracted) with increasing (filled circles) and decreasing (open triangles) voltage at 122°C (frequency $f = 50$ Hz). The cell was cooled from the isotropic phase without a voltage applied.

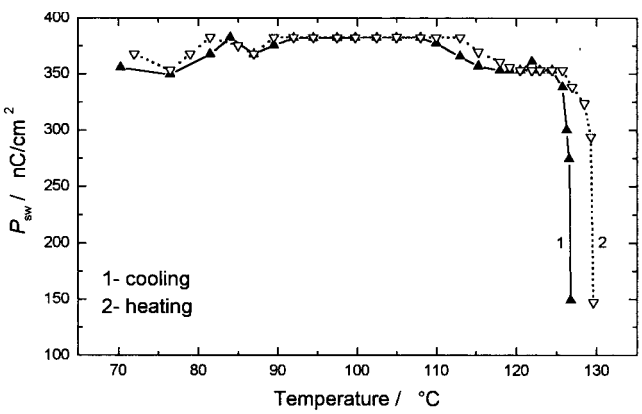

Figure 5. Temperature dependence of switched polarization on heating (open triangles) and cooling (closed triangles). Voltage amplitude $U_m = \pm 95$ V, $f = 50$ Hz.

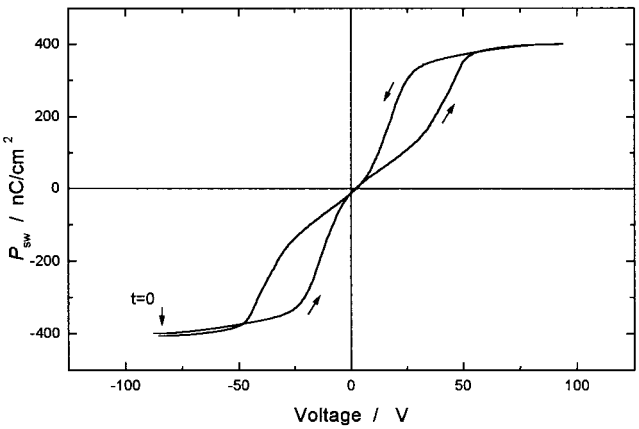

Figure 8. An example of the hysteresis curve obtained by integrating repolarization curve. Triangular waveform, $U_m = \pm 90$ V, $f = 50$ Hz, $T = 123.5°C$. The cell was cooled from the isotropic phase without field applied.

As observed earlier [16], at low fields the two loops are very close to each other, showing polarization switching almost without threshold. It appears that for the switching of a banana-shaped compound there is a very low (if any) potential barrier between the initial antiferroelectric and final ferroelectric states.

In principle, the widths of the individual current peaks shown in figure 3(*b*) contain information about partial viscosities of the two sub-systems switched. Returning to the table we can see that the width (on average $w_{in} = 0.7$ ms) of the two inner peaks 2 and 4 (even without contribution of peak 3) is considerably larger than the width of the outer peaks 1 and 5 ($w_{out} \approx 0.4$ ms). For conventional liquid crystal ferroelectrics the rotational viscosity γ can easily be found from the height of the current peak maximum observed at a certain amplitude U of triangular voltage shape [17]. Unfortunately there is no corresponding theory for antiferroelectrics. We can only try to estimate the ratio γ_{in}/γ_{out} for the two groups of current peaks, inner and outer, discussed above; because, from a general point of view, the width of the peaks must be proportional to the switching time τ, which in turn is proportional to $\gamma/\mathbf{P}_s\mathbf{E}$. The applied voltage is different from the inner and outer peaks, therefore $\gamma_{in}/\gamma_{out} = w_{in}\mathbf{P}_{in}U_{in}/w_{out}\mathbf{P}_{out}U_{out}$. Taking from the table the values of $\mathbf{P}_{in} = 199$ nC cm^{-2}, $U_{in} = 23$ V and $\mathbf{P}_{out} = 151$ nC cm^{-2}, $U_{out} = 37$ V we obtain $\gamma_{in}/\gamma_{out} = 1.4$. Assuming peak 3 belongs to the inner group, the same ratio would reach the value of about 2.

From our experiments we may conclude that the 'inner peak system' is related to a markedly slower process than its outer counterpart. For other banana-shaped compounds it has been found from electro-optical experiments [13, 16] that the chiral domains switch more slowly than the racemic ones. Therefore, it is reasonable to assume that, in our case, the inner and outer peaks correspond to homogeneously chiral and racemic domains, respectively.

The absolute measurement of rotational viscosity has been carried out using a square-wave form of voltage. The repolarization current oscillograms are shown in figure 9 for different temperatures. No structure is seen in the oscillogram, therefore from the width w of a current maximum at its half-height, with the simplest relationships known for ferroelectrics [18], we can calculate only the average switching time $\tau = w/2$ and average rotational viscosity $\gamma = \tau\mathbf{P}_s\mathbf{E}$. The temperature dependence of $\tau(T)$ is shown in the inset in figure 9. With data for $\mathbf{P}_s$ taken from figure 5, the calculated values of $\gamma(1/T)$ are plotted in figure 10. On decreasing temperature from 125 to 90°C the γ values increase from 0.2 to 0.6 Pa s (2–6 Poise). A similar value (≅0.1 Pa s at 135°C if one

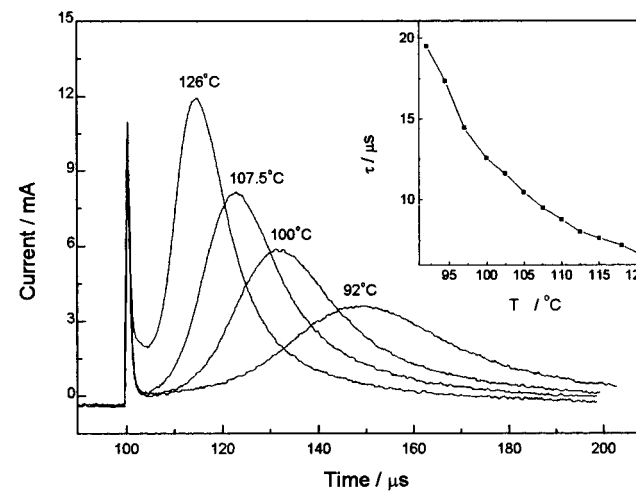

Figure 9. Temperature dependent oscillograms of the repolarization current obtained with square-wave form of voltage $U_m = \pm 90$ V, $f = 50$ Hz. Inset: switching time as a function of temperature.

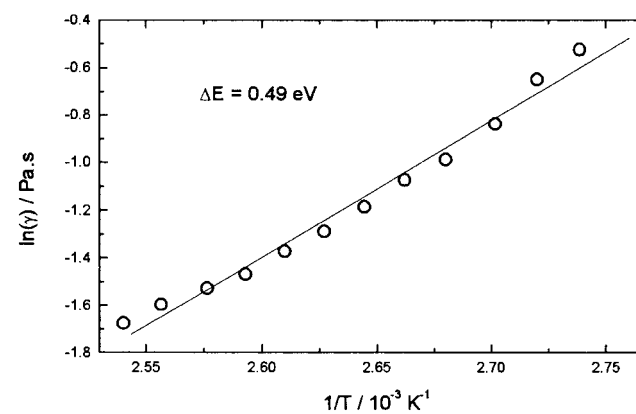

Figure 10. Logarithm of average rotational viscosity as a function of inverse temperature in the B_2 phase of the banana-shaped compound studied.

disregards an extra factor 2 in formula for γ) has been found by Heppke *et al.* [16] for another banana-shaped compound. The temperature slope of $\ln(\gamma)$ gives an activation energy $\Delta E = 0.49$ eV.

5. Conclusion

We have performed a detailed study of the field induced polarization switching of the antiferroelectric B_2 phase of a banana-shaped compound, the tetradecyl homologue ($n = 14$) of the series 2-chloro-1,3-phenylene bis[4-(4-*n*-alkylphenylimino)benzoates]. The fine structure of the current response oscillograms found in a certain temperature range was attributed to the field switching of two antiferroelectric subsystems, namely the racemic and homogeneously chiral domains which appear as a result of the spontaneous breaking of mirror symmetry. The two subsystems have different threshold voltages for switching and different switching times. The average rotational viscosity (0.2–0.6 Pa s) was measured in a wide temperature range of the B_2 phase and showed activation energy about 0.49 eV.

This work is supported by RFBR grant No. 99-02-176484, by the Deutsche Forschungsgemeinschaft and by the Fond der Chemischen Industrie.

References

[1] Tournilhac, F., Blinov, L. M., Simon, J., and Yablonsky, S. V., 1992, *Nature*, **359,** 621.
[2] Niori, T., Sekine, T., Watanabe, J., Furukawa, T., and Takezoe, H., 1996, *J. mater. Chem.*, **6,** 1231.
[3] Soto Bustamante, E. A., Yablonskii, S. V., Ostrovskii, B. I., Beresnev, L. A., Blinov, L. M., and Haase, W., 1996, *Liq. Cryst.*, **21,** 829.
[4] Weissflog, W., Lischka, Ch., Benne, T., Scharf, T., Pelzl, G., Diele, S., and Kruth, H., 1997, *Proc. SPIE*, **3319,** 14.
[5] Walba, D. M., Körblova, E., Shao, R., Maclennan, J. E., Link, D. R., and Clark, N. A., 2000, *Science*, **288,** 2181.
[6] Meyer, R., Liebert, L., Strzelecki, L., and Keller, P., 1975, *J. Phys. (Fr.) Lett.*, **36,** L69.
[7] Fukuda, A., Takanishi, Y., Isozaki, T., Ishikawa, K., and Takezoe, H., 1994, *J. mater. Chem.*, **4,** 997.
[8] Blinov, L. M., 1998, *Liq. Cryst.*, **24,** 143.
[9] Link, D. R., Natale, G., Shao, R., Maclennan, J. E., Clark, N. A., Körblova, E., and Walba, D. M., 1997, *Science*, **278,** 1924.
[10] Pelzl, G., Diele, S., and Weissflog, W., 1999, *Adv. Nat.*, **11,** 707.
[11] Watanabe, J., Niori, T., Choi, S.-W., Takanishi, Y., and Takezoe, H., 1998, *Jpn. J. appl. Phys. 2*, **37,** L401.
[12] Weissflog, W., Lischka, Ch., Diele, S., Pelzl, G., and Wirth, I., 1999, *Mol. Cryst. liq. Cryst.*, **328,** 101.
[13] Zennoji, M., Takanishi, Y., Ishikawa, K., Thisayukta, J., Watanabe, J., and Takezoe, H., 2000, *Jpn. J. appl. Phys. 1*, **39,** 3536.
[14] Ngyuen, H. T., Rouillon, J. C., Marcerou, J. P., Bedel, J. P., Barois, P., and Sarmento, S., 1999, *Mol. Cryst. liq. Cryst.*, **328,** 177.
[15] Miyasato, K., Abe, S., Takezoe, H., Fukuda, A., and Kuze, E., 1983, *Jpn. J. appl. Phys.*, **22,** L661.
[16] Heppke, G., Jakli, A., Rauch, S., and Sawade, H., 2000, *Phys. Rev. E*, **60,** 5575.
[17] Escher, C., Geelhaar, T., and Böhn, E., 1999, *Liq. Cryst.*, **3,** 469.
[18] Lagerwall, S. T., 1999, *Ferroelectric and Antiferroelectric Liquid Crystals* (Weinheim: Wiley-VCH).